Noname manuscript No.
(will be inserted by the editor)

Performance and ASIC Designs of the K-best LSD and LMMSE Detectors for LTE Downlink

Essi Suikkanen · Markku Juntti

Received: date / Accepted: date

Abstract We consider performance comparison and application specific integrated circuit (ASIC) designs of linear minimum mean-square error (LMMSE) and K-best list sphere detector (LSD) algorithms for 4×4 and 8×8 multiple-input multiple-output (MIMO) orthogonal frequency division multiplexing (OFDM) systems. Requirements for higher data rate and lower power consumption set new challenges for implementation. In order to minimize the power consumption, an optimal detector would be able to switch the detection algorithm to suit the channel conditions. The detectors are designed for three different modulation schemes using 28 nm complementary metal oxide semiconductor (CMOS) technology. The communications performance is evaluated in the Third Generation Partnership Project (3GPP) Long-Term Evolution (LTE) system. The impact of transmit precoding is considered. The ASIC designs aim at providing the hardware design aspects to the comparison of detectors. The designs are synthesized and complexity and power consumption results are found. Based on the ASIC synthesis and communications performance results, we show the performance–energy efficiency and performance–complexity comparison. We also present the most suitable scenarios for a low-power detector and show how the transmit precoding impacts the detector selection.

Keywords LTE · MIMO–OFDM · adaptive detection · LMMSE · K-best LSD · ASIC

1 Introduction

The Third Generation Partnership Project (3GPP) Long-Term Evolution (LTE) standard [1] uses a combination of multiple-input multiple-output (MIMO) and orthogonal frequency division multiplexing (OFDM), to offer better performance in terms of capacity, diversity and bandwidth efficiency. The receivers for MIMO–OFDM systems need to be capable to cope with interference caused by spatial multiplexing or inter-antenna interference. Detection algorithms with high detection rate, low computational complexity and low power consumption need to be designed. Based on our observations, the detector is one of the most power hungry parts of the wireless receiver. Therefore, it would be advantageous to switch between simple and complex detection algorithms based on the channel state, in order to save energy.

Adaptation of the detection algorithm is not a straightforward matter. The communication performance depends on the channel conditions which can change rapidly due to the movement of the mobile, scattering or other factors in the propagation environment. Also the channel estimation performance, transmit precoding and hybrid automatic repeat request (HARQ) have different impacts on different detection algorithms, which has to be taken into consideration.

The comparison between different detection algorithms should take into account both, the communications performance and the hardware implementation

This research was financially supported in part by Tekes, the Finnish Funding Agency for Innovation, Academy of Finland, Nokia Solutions and Networks, Broadcom Communications Finland and Xilinx.

Essi Suikkanen
Keysight Technologies Finland Oy,
Elektroniikkatie 10, FIN-90590 Oulu, Finland
E-mail: essi.suikkanen@keysight.com

Markku Juntti
Centre for Wireless Communications,
P.O. Box 4500, FIN-90014 University of Oulu, Finland
E-mail: markku.juntti@oulu.fi

aspects. Even if the detection rate supported by the implementation of a low-complexity detector is high, poor channel conditions may impair the overall performance of the detector. A more complex receiver, on the other hand, could reach the data rate requirements with satisfactory quality of service. The handheld devices nowadays are required to support a wide class of services with high quality, and usually the algorithms that deliver the best performance have the highest complexity and power consumption. With careful architecture design, also the complex algorithms can become competitive compared to the simple ones. Nevertheless, the usual case is that the cost of high performance is high power consumption. By combining the implementation and the performance results of different detection algorithms, the scenarios where acceptable performance can be reached while keeping the energy consumption low, can be recognized. Also the scenarios that require a complex detector can be recognized, and some other strategy for power saving can be designed for them.

Adaptive detection for MIMO systems was proposed in [2], where a low complexity detector was chosen for a channel with low spatial correlation and a more complex detector was applied for an ill-conditioned channel. Receiver with the maximum likelihood (ML) and linear minimum mean-square error (LMMSE) detectors was studied in [3]. The complexity of the chosen algorithms was discussed, but no actual hardware implementation results were given. It was shown by simulations that the proposed adaptive detection scheme provides a trade-off between the performance and complexity in 4×2 MIMO system.

An adaptive MIMO detector including the maximum ratio combining (MRC), LMMSE and successive interference cancellation (SIC) algorithms was implemented in [4] using partially reconfigurable application-specific instruction-set processors (rASIP). Different modulation schemes and antenna configurations were supported. Hardware synthesis results were provided, but the performance of the algorithms on the system level was not shown. Reconfigurable ASIP was also used in [5], where zero forcing (ZF), LMMSE, SIC and Markov chain Monte Carlo (MCMC) detectors were implemented using 65 nm complementary metal oxide semiconductor (CMOS) technology. It was shown that the proposed design is more efficient than other flexible designs and has throughput that approaches the dedicated ASIC designs, but the communications performance was not addressed.

Adaptive detection can also be realized by using only one detection algorithm. An adaptive hard output K-best list sphere detector (LSD) was implemented in [6]. The list size K was adapted from 1 to 5, based on the channel signal-to-noise ratio (SNR). The channel quality indicator (CQI) [7] was used to adapt the clock-gating in the detector. The implementation was done using 22 nm CMOS technology and to support 4×4 MIMO and binary phase shift keying (BPSK) to 16 quadrature amplitude modulation (QAM). It was shown that energy reduction can be achieved by adapting the list size. Adaptive LMMSE detection was considered in [8] for 8×8 MIMO system. The Doppler frequency was monitored and the clock frequency and supply voltage were adjusted according to the chosen computational speed. The detection of a packet was skipped if the receiver detected low Doppler frequency indicating a slowly changing channel.

We compared the performances of the LMMSE, SIC, K-best LSD and selective spanning with fast enumeration (SSFE) detectors in 4×4 MIMO–OFDM system with precoding and HARQ in [9] and [10]. The SIC detector was shown to suffer from error propagation in poor channel conditions. The SSFE detector was unable to outperform the K-best LSD and was occasionally outperformed by the LMMSE detector. The performances of the LMMSE and K-best detectors in 4×4 and 8×8 MIMO–OFDM systems with HARQ were compared in [11]. The performance–energy efficiency comparison between the K-best LSD and LMMSE detector were presented in [12] for the 4×4 and 8×8 systems with HARQ.

In this paper, we study the performance, complexity and energy efficiency of the K-best LSD and LMMSE detectors with and without transmit precoding. The LMMSE and K-best LSD were chosen as the candidate algorithms for an adaptive detector based on our previous studies. The LMMSE is a relatively low complexity MIMO detection algorithm, which is usually considered as the basic benchmark solution. However, its performance degrades in difficult channel conditions, which means roughly that the number of "strongly nonzero" singular values of the channel matrix is smaller than the number of spatially multiplexed data streams [13]. The K-best LSD is a breadth-first tree-search algorithm [14], which keeps K nodes with the smallest accumulated Euclidean distances at each level of the tree. The K-best LSD offers good performance and is considered to be a near maximum likelihood (ML) detector with large enough K. However, high modulation order, list size, and the number of antennas increase the complexity of the LSD making it infeasible for the low power receivers. Also a depth-first sphere decoding (SD) [15] could be considered as it provides lower bit error rate than the breadth-first detector. However, the throughput of the depth-first SD is not constant and due to the sequential search order, the architecture is difficult

to parallelize. The breadth-first SD provides deterministic throughput as well as the fixed-throughput sphere decoder (FSD) implemented in [16] and [17]. Here the breadth-first approach was chosen.

The results give a solid basis for recognizing the scenarios where a simple, low-power detector can be used. The ASIC synthesis results are obtained using 28 nm CMOS technology and include dedicated architectures for 4×4 and 8×8 cases with the quadrature phase shift keying (QPSK), 16-QAM and 64-QAM constellations. The ASIC designs aim at meeting the detection rate requirements in LTE, and provide the hardware implementation aspect to the comparison. The simulations in the 3G LTE system give information on the communications system performance of the chosen detectors. The performance is characterized by data transmission throughput, which is defined to be equal to the nominal information transmission rate of successfully received information bits, R_b, times (1 – frame error rate (FER)).

$$\text{Throughput} = R_\mathrm{b} * (1 - \text{FER}) \tag{1}$$

The data transmission throughput reflects the reliability of the decisions. The ASIC synthesis results include latency, power consumption and complexity, which is given as equivalent gates. The latency is transformed to detection rate (Eq. 6), which represents the rate by which the algorithm is able to make data decisions. The goodput, which is the minimum of the data transmission throughput and the hardware detection rate of information bits, is computed to combine the reliability and hardware limitations of the algorithms. Based on the goodput, the recommendations on scenarios suitable for low-power detector are given and also the performance–complexity and performance–energy efficiency tradeoffs are shown. The use of different CMOS technologies, clock frequencies, and tools makes it complicated to compare the achieved results to the literature. Therefore we do not provide a comparison to any baseline system, but compare the results to a case where only one of the implemented detectors would be used.

The paper is organized as follows. The system model is presented in Section II, including channel estimation, hybrid automatic repeat request (HARQ) and precoding. In Section III, the performance comparison based on simulations is shown with and without precoding. In Section IV, we provide top-level architectures and ASIC synthesis results of the algorithms. The performance and implementation results are combined in Section V and the performance–energy efficiency and performance–complexity comparisons are given. The conclusions are drawn in Section VI.

2 System Model

We consider an OFDM based downlink MIMO spatial multiplexing transmission system using N_T transmit and N_R receive antennas, where $N_\mathrm{T} = N_\mathrm{R}$ and N_T data streams are multiplexed over N_T transmit antennas. A maximum of two separately encoded data streams is specified in the LTE standard [1]. Horizontal encoding is used, which means that two streams of data bits are encoded separately and then mapped onto different layers. The system model is illustrated in Fig. 1.

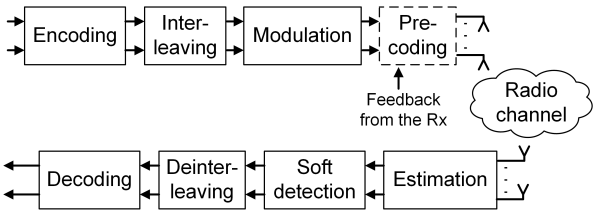

Fig. 1 System model.

The received frequency domain signal for each OFDM subcarrier p at discrete time index t is given as

$$\mathbf{y}_p(t) = \mathbf{H}_p(t)\mathbf{x}_p(t) + \mathbf{n}_p(t), p = 1, 2, ..., P, \tag{2}$$

where $\mathbf{y}_p \in \mathbb{C}^{N_\mathrm{R}\times1}$, $\mathbf{x}_p \in \mathbb{C}^{N_\mathrm{T}\times1}$, and $\mathbf{n}_p \in \mathbb{C}^{N_\mathrm{R}\times1}$ are the received signal, the transmitted signal, and the complex zero-mean Gaussian noise vector with noise variance σ^2, respectively, for subcarrier p. $\mathbf{H}_p \in \mathbb{C}^{N_\mathrm{R}\times N_\mathrm{T}}$ is the channel matrix for subcarrier p. Bit interleaved coded modulation (BICM) is applied and the entries of $\mathbf{x}_p$ are chosen independently from a complex QAM constellation Ω with sets of Q transmitted information bits $\mathbf{b} = [b_1, ..., b_Q]^\mathrm{T}$ per symbol, i.e. $|\Omega| = 2^Q$. The set of possible transmitted symbol vectors is Ω^{N_T}. In the following equations the subcarrier index p and time index t are omitted for the sake of clarity.

The real-valued representation of the system is given as

$$\underbrace{\begin{bmatrix}\Re\{\mathbf{y}\}\\ \Im\{\mathbf{y}\}\end{bmatrix}}_{\mathbf{y}_\mathrm{r}} = \underbrace{\begin{bmatrix}\Re\{\mathbf{H}\} & -\Im\{\mathbf{H}\}\\ \Im\{\mathbf{H}\} & \Re\{\mathbf{H}\}\end{bmatrix}}_{\mathbf{H}_\mathrm{r}} \underbrace{\begin{bmatrix}\Re\{\mathbf{x}\}\\ \Im\{\mathbf{x}\}\end{bmatrix}}_{\mathbf{x}_\mathrm{r}} + \underbrace{\begin{bmatrix}\Re\{\mathbf{n}\}\\ \Im\{\mathbf{n}\}\end{bmatrix}}_{\mathbf{n}_\mathrm{r}}, \tag{3}$$

where $\mathbf{y}_\mathrm{r} \in \mathbb{R}^{2N_\mathrm{R}\times1}$, $\mathbf{H}_\mathrm{r} \in \mathbb{R}^{2N_\mathrm{R}\times2N_\mathrm{T}}$, $\mathbf{x}_\mathrm{r} \in \mathbb{Z}^{2N_\mathrm{T}\times1}$ and $\mathbf{n}_\mathrm{r} \in \mathbb{R}^{2N_\mathrm{R}\times1}$. $\Re\{\cdot\}$ and $\Im\{\cdot\}$ denote the real part and the imaginary part of their arguments, respectively. The real-valued system model doubles the matrix dimensions and limits the choice of constellations, but all the 3GPP LTE modulation methods can be supported by real valued system model based detector design. On the other hand, getting rid of the complex numbers simplifies some calculations. For example, the Euclidean distance calculation is simpler in the real-valued system

than in the complex-valued one [18] and the selection of the closest constellation point can be done in one dimension.

For the implementations we consider a MMSE extended real-valued system, which can improve the detection quality [19]. Now the channel matrix $\mathbf{H}_\mathrm{e} \in \mathbb{R}^{(2N_\mathrm{R}+2N_\mathrm{T})\times 2N_\mathrm{T}}$ and the received signal $\mathbf{y}_\mathrm{e} \in \mathbb{R}^{(2N_\mathrm{R}+2N_\mathrm{T})\times 1}$ are given as

$$\mathbf{H}_\mathrm{e} = \begin{bmatrix} \mathbf{H}_\mathrm{r} \\ \sigma \mathbf{I}_{2N_\mathrm{T}} \end{bmatrix} \qquad \mathbf{y}_\mathrm{e} = \begin{bmatrix} \mathbf{y}_\mathrm{r} \\ \mathbf{0}_{2N_\mathrm{T}\times 1} \end{bmatrix}. \tag{4}$$

In the sequel, the MMSE extended real-valued system is assumed in the ASIC designs, and, therefore the subindices r and e are omitted.

2.1 Channel Estimation

We assume pilot aided transmission, where pilot symbols known at the receiver are used to estimate the channel [20]. The length of the channel and the tap delays are assumed to be known in the case of 4×4 transmission. In the 4×4 system, the received time domain signal is transformed into frequency domain with a FFT before estimation. After the channel estimation, the channel impulse response result from the least squares (LS) estimator is transformed into frequency domain using a second FFT.

The frequency domain LS estimator proposed in [21] is used for the 8×8 system. The received transmission time interval (TTI) consisting of 14 OFDM symbols is buffered, and after the whole TTI is received and the channel estimate is computed, detection and decoding are performed.

2.2 HARQ and Precoding

HARQ [22, 23] based on the Chase combining is used with maximum of three retransmissions. An error-free feedback channel is assumed. In the HARQ scheme, if the transmitted data packet is received erroneously, the erroneous packet is saved and retransmission of the same data is requested. The erroneous packet and the data from the retransmission are combined and decoded. The retransmission continues until the data are received successfully or the maximum number of retransmissions is reached. HARQ enables more reliable communication, but the latency of the system is increased, because the transmitter sends one packet at a time and waits for an acknowledgement from the receiver before sending new data. In this work, the data packet is considered to be one TTI. The whole TTI is retransmitted if there is even one erroneously received OFDM symbol in it.

The LTE-Advanced (LTE-A) codebook based precoding [1] is considered in the case of 4×4 transmission system and only the data symbols are precoded. In the 8×8 system, the pilots are precoded with the same precoder as the data. The estimated channel includes the combined effect of the precoding and the radio channel. Instead of designing the precoders, we consider a codebook proposed by ZTE [24].

The precoding matrix $\mathbf{P}$ with the highest instantaneous capacity value is chosen. It is calculated for pth subcarrier as

$$C_p = \log(\det(\mathbf{I} + \frac{E_s}{\sigma^2 N_\mathrm{R}} (\mathbf{H}_p\mathbf{P})^\mathrm{H}(\mathbf{H}_p\mathbf{P}))), \tag{5}$$

where E_s is the symbol energy and $\mathbf{I}$ is an identity matrix. Capacity is summed over the subcarriers in the OFDM symbol. The precoding matrix is adapted once in a TTI and is the same for all the subcarriers in a symbol.

3 Performance Comparison

The simulation results presented in [9–12] show that in an uncorrelated channel, the LMMSE detector is able to outperform the K-best LSD, but as the correlation increases, the opportunities to use the LMMSE detector become scarce. In the 8×8 MIMO system, the LMMSE detector is unable to separate all the spatial streams, and, therefore, it is performing poorly compared to the K-best LSD. Here we show how the precoding impacts the detector selection in adaptive detection, when only the simple LS based channel estimation is used.

3.1 Simulation Parameters

The simulation parameters are based on the LTE standard [1] and the Typical Urban (TU) channel model based on the 3GPP vehicular A model [25] is applied. The simulation and channel model parameters are given in Table 1. The same parameter choices have been used in the authors' earlier work and are, therefore, used also here to allow easier comparison to previous results. Each SNR point corresponds to a transmission of 28000 OFDM symbols and the mobile speed is set to 3 km/h. The number of turbo decoder iterations was set to 8.

The channel spatial correlation matrix can be obtained from $\mathbf{C}_\mathrm{TX} \otimes \mathbf{C}_\mathrm{RX}$, where $\mathbf{C}_\mathrm{TX}$ and $\mathbf{C}_\mathrm{RX}$ are the spatial correlation matrices for the transmitter and the receiver, respectively, and $\otimes$ is the Kronecker product. The base station (BS) azimuth spread affects the spatial

correlation matrix of the transmitter. The channel with BS azimuth spread of 5° is considered as a moderately correlated channel, and with 2° as a highly correlated channel. Also a spatially uncorrelated channel is considered.

The data transmission throughput is computed as the nominal information transmission rate of successfully received information bits times (1 – FER). In other words, the results report the reliable and useful data transmission capability supported by the detector and the applied MIMO configuration, modulation and coding. One frame is considered to be one TTI, which equals 14 OFDM symbols. In the HARQ scheme, if the transmitted data is received erroneously, the erroneous TTI is saved and a retransmission of the same data is requested. If the maximum number of retransmissions is reached without successful reception, the whole TTI is discarded.

Table 1 Simulation and Channel Model Parameters

Simulation parameters	
Coding	Turbo coding with 1/2 code rate
Number of subcarriers	512 (300 used)
Bandwidth	5 MHz
Symbol duration	71.4 μs
Duration of one TTI	14 OFDM symbols
Modulation	4-QAM, 16-QAM and 64-QAM
Channel model	TU vehicular A
User velocity	3 km/h
Channel model parameters	
Number of paths	6
Path delays	[0...2510] ns
Path power	[0...-20] dB
BS antenna spacing	4 λ
MS antenna spacing	0.5 λ
BS average angle of departure	20°
MS average angle of arrival	67.5°
BS azimuth spread	2° / 5°
MS azimuth spread	35°

3.2 Simulation Results

The data transmission throughput versus SNR for the 4×4 system without precoding in an uncorrelated channel is shown in Fig. 2, in a moderately correlated channel in Fig. 3 and in a highly correlated channel in Fig. 4. The data transmission throughput with the same antenna setup and with precoding in an uncorrelated channel is shown in Fig. 5, in a moderately correlated channel in Fig. 6 and in a highly correlated channel in Fig. 7. The LS channel estimation is used. The precoding enhances the performance at the lower SNR regime, especially for the LMMSE detector. Even without the precoding, the LMMSE detector can outperform or provide similar throughput as the K-best LSD in an uncorrelated channel. As the spatial correlation increases, the LMMSE detector cannot compete with the K-best LSD, even if the precoding is used.

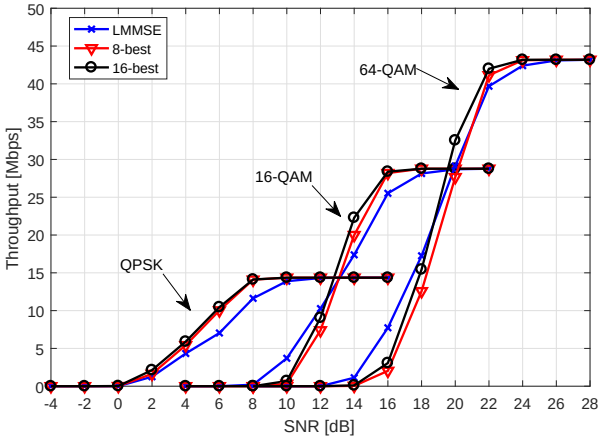

Fig. 2 Throughput of the LMMSE and K-best detectors vs. SNR in 4×4 system without precoding, uncorrelated channel.

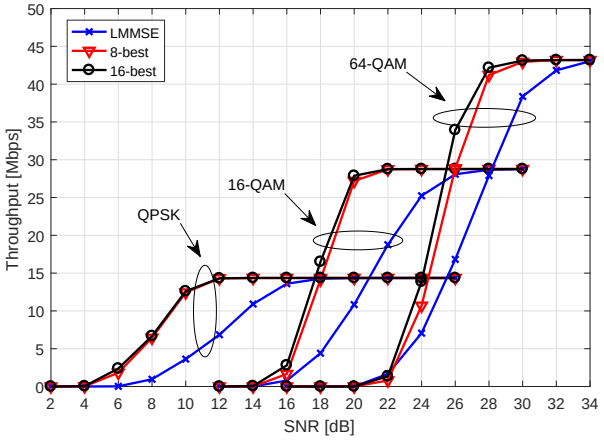

Fig. 3 Throughput of the LMMSE and K-best detectors vs. SNR in 4×4 system without precoding, moderately correlated channel.

The data transmission throughput versus SNR for the 8 × 8 system without the precoding in an uncorrelated channel is shown in Fig. 8, in moderately correlated channel in Fig. 9 and in highly correlated channel in Fig. 10. The data transmission throughput versus SNR for the same antenna setup with precoding in an uncorrelated channel is shown in Fig. 11, in moderately correlated channel in Fig. 12 and in highly correlated

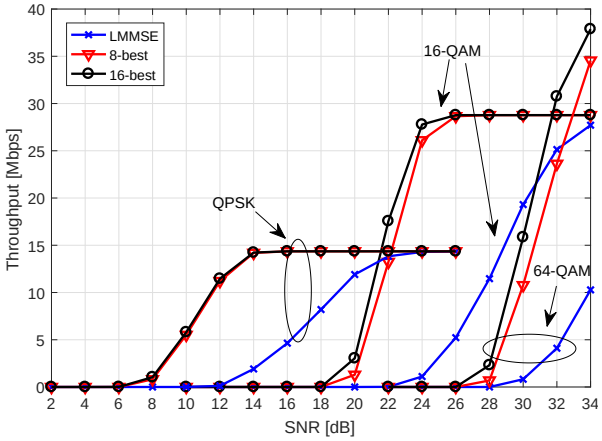

Fig. 4 Throughput of the LMMSE and K-best detectors vs. SNR in 4×4 system without precoding, highly correlated channel.

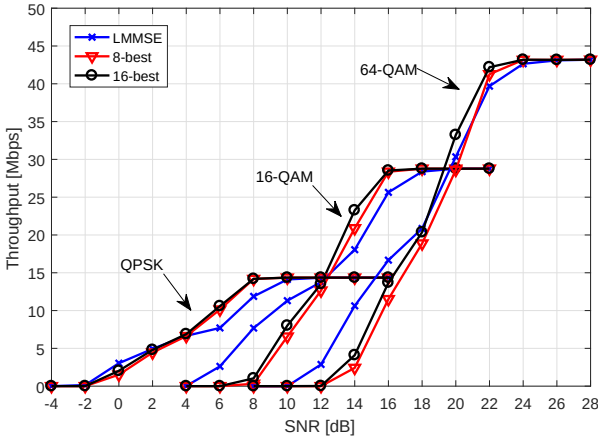

Fig. 5 Throughput of the LMMSE and K-best detectors vs. SNR in 4×4 system with precoding, uncorrelated channel.

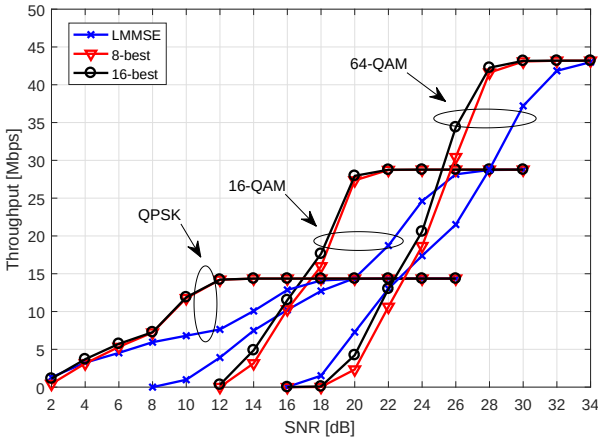

Fig. 6 Throughput of the LMMSE and K-best detectors vs. SNR in 4×4 system with precoding, moderately correlated channel.

channel in Fig. 13. The effect of precoding is similar to the case of 4×4 system and the precoding improves the throughput especially on the low SNR regime. However,

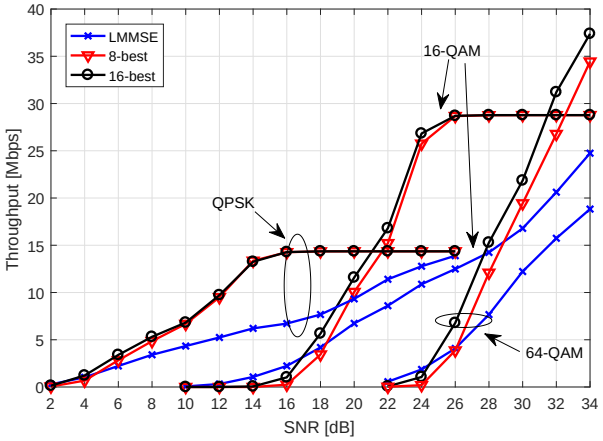

Fig. 7 Throughput of the LMMSE and K-best detectors vs. SNR in 4×4 system with precoding, highly correlated channel.

as the SNR increases, the performance of the LMMSE detector with precoding degrades compared to the performance without precoding for 16-QAM and 64-QAM. Similar, but not as significant, effect can be seen with the K-best LSD. Also in the 4×4 system with high spatial correlation and 16-QAM, precoding degrades the performance of the LMMSE detector at the high SNRs, as can be observed from Fig. 7. We have concluded the reason to be that the capacity based selection of the precoder is not suitable for the high SNRs. The K-best LSD is able to handle the deteriorated effective channel **HP**, but the LMMSE cannot do the same.

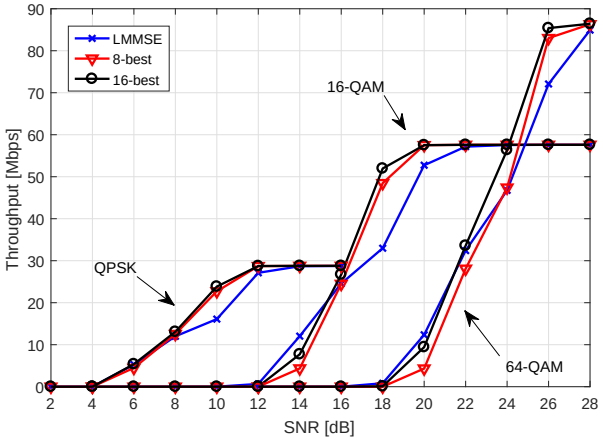

Fig. 8 Throughput of the LMMSE and K-best detectors vs. SNR in 8×8 system without precoding, uncorrelated channel.

4 ASIC Design Comparison

The simulation results show the communications performance of the chosen algorithms. In order to obtain

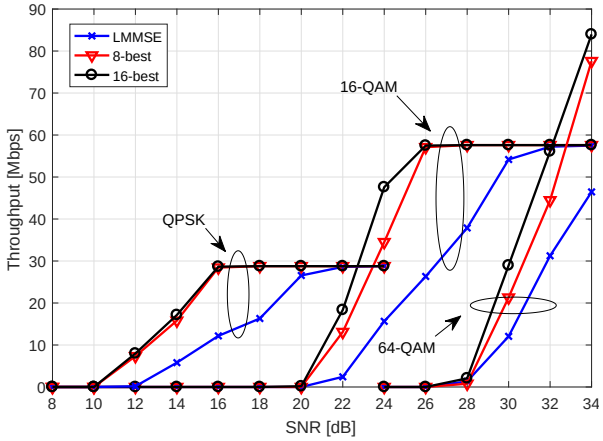

Fig. 9 Throughput of the LMMSE and K-best detectors vs. SNR in 8×8 system without precoding, moderately correlated channel.

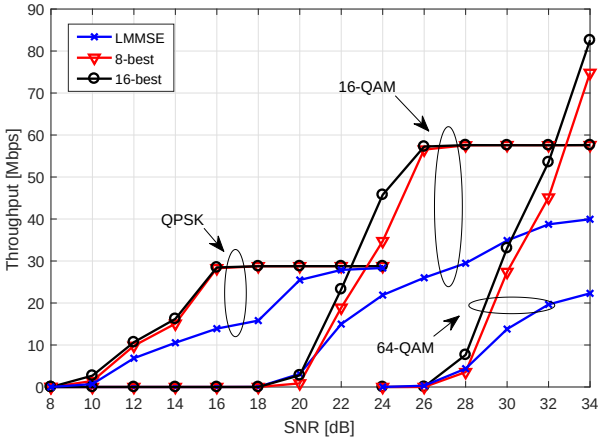

Fig. 12 Throughput of the LMMSE and K-best detectors vs. SNR in 8×8 system with precoding, moderately correlated channel.

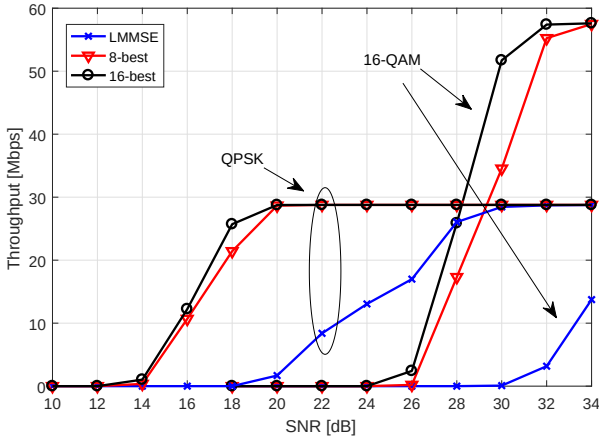

Fig. 10 Throughput of the LMMSE and K-best detectors vs. SNR in 8×8 system without precoding, highly correlated channel.

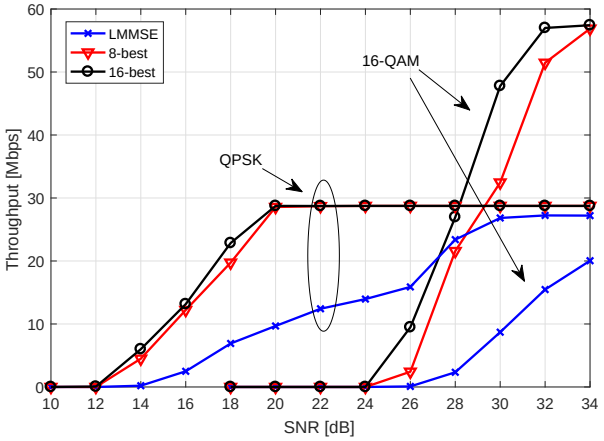

Fig. 13 Throughput of the LMMSE and K-best detectors vs. SNR in 8×8 system with precoding, highly correlated channel.

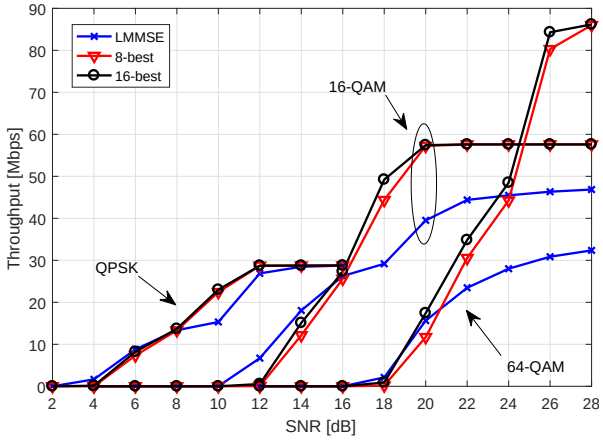

Fig. 11 Throughput of the LMMSE and K-best detectors vs. SNR in 8×8 system with precoding, uncorrelated channel.

a perspective to the hardware implementation aspects of the detectors, ASIC synthesis results are presented. The Cadence C-to-Silicon Compiler High-Level Synthesis (HLS) tool [26], which synthesizes algorithms written in SystemC into hardware, was used in this work to produce the register transfer level (RTL) models. The logic synthesis of the RTL model to gate-level netlist was done using the Synopsys Design Compiler [27] and 28 nm CMOS technology. The clock frequency was set to 769 MHz for all detectors and with this frequency the HLS tool was able to produce all of the RTL models with the given timing requirements.

The fixed point word lengths and the number of integer bits were determined through simulations. Comparison to the floating point word lengths was made to ensure that the chosen word lengths did not degrade the performance. The word lengths for the K-best implementations ranged from 12 to 16 depending on the modulation order. For the LMMSE, the inversion of $\mathbf{R}$ required word lengths of 22 bits. For the LLR computation, word lengths from 12 up to 18 were used depending on the modulation order.

We assume 7 OFDM symbols in a 0.5 ms slot [1]. With 20 MHz bandwidth there are 1200 data subcarriers in one OFDM symbol, which means that during one slot, 8400 subcarriers have to be processed. The pilot overhead is approximately 14.3% in the 4×4 and 8×8 MIMO systems. Because the pilot subcarriers do not need to be detected, the time to process one subcarrier is approximately 69 ns.

The latency of an algorithm is transformed into hardware detection rate, which represents the rate by which the algorithm is able to make data decisions. It tells nothing about the reliability of the decisions. The detection rate is computed as

$$R_{det} = \frac{QN_{\mathrm{T}}}{D_{\mathrm{tp}}}\mathrm{Mbps}, \tag{6}$$

where Q is the number of bits per symbol and D_{tp} is the throughput latency. The used HLS tool provides the latency for every detector architecture considering also pipelining. In the computation of the required detection rates, the pilot overhead is taken into account. The algorithm performance is evaluated by computing the goodput [28], which is defined to be the minimum of the detection rate and the data transmission throughput. In this way, also the reliability of the decisions is taken into account.

All division operations needed in the detectors are approximated using the Newton-Raphson iterations [29] given as

$$z^{(n)} = z^{(n-1)}(2 - cz^{(n-1)}), n = 1, ..., N_{\mathrm{iter}}, \tag{7}$$

where N_{iter} is the number of iterations and $\lim_{n\to\infty} z^{(n)} = c^{-1}$. The number of iterations needed and a suitable initial guess, $z^{(0)}$, were determined by simulations.

The K-best LSD and the LMMSE detector utilize the $\mathbf{Q}$ and $\mathbf{R}$ matrices from the QR decomposition (QRD). The QRD decomposes the MMSE extended real-valued channel (4) into an upper triangular matrix $\mathbf{R} \in \mathbb{R}^{2N_{\mathrm{T}} \times 2N_{\mathrm{T}}}$ and an orthogonal matrix $\mathbf{Q} \in \mathbb{R}^{(2N_{\mathrm{R}}+2N_{\mathrm{T}}) \times 2N_{\mathrm{T}}}$. [30] The complexity of the QRD is the same for both detection algorithms and therefore it is not included in the implementations. The QRD is performed once during the channel coherence time.

The results are presented in gate equivalents (GE) and power consumption estimates. The latencies of the detectors are presented as clock cycles (cc).

4.1 K-best LSD

4.1.1 Architecture

The top-level architecture of the K-best LSD receiver is presented in Fig. 14. The grey boxes represent the operations that have to be performed for every data subcarrier. The operations in the white boxes need to be computed only once in a channel coherence time.

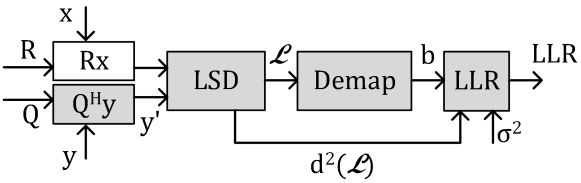

Fig. 14 The top-level architecture of the K-best LSD receiver.

After the QRD, the possible transmitted symbols, $\mathbf{x}$, are multiplied with $\mathbf{R}$ and the received signal $\mathbf{y}$ is multiplied with $\mathbf{Q}$ as $\mathbf{y}' = \mathbf{Q}^{\mathrm{H}}\mathbf{y}$. The squared partial Euclidean distances (PED), d, are computed as

$$d(\mathbf{x}_i^{N_{\mathrm{T}}}) = \sum_{j=i}^{N_{\mathrm{T}}} |y'_j - \sum_{l=j}^{N_{\mathrm{T}}} r_{j,l}x_l|^2, i = N_{\mathrm{T}}, ..., 1, \tag{8}$$

where y'_j is the jth element of $\mathbf{y}'$, $r_{j,l}$ is the j,lth element of $\mathbf{R}$, x is the lth element of the candidate vector $\mathbf{x}_i^N$ and $\mathbf{x}_i^N$ denotes the last $N - i + 1$ elements of vector $\mathbf{x}$ [31]. The PEDs are sorted in the LSD block and the final candidate symbol list, $\mathcal{L}$, is demapped to a binary form, $\mathbf{b}$, and the log-likelihood ratios (LLR) are computed from the list of candidates and their PEDs $d^2(\mathcal{L})$. The simplified method to compute the LLRs is used as shown in [28]. The range of LLRs is limited to reduce the required list size [32]. The sorters are insertion sorters. In the case of QPSK, sorting is not needed on every stage which decreases the complexity.

The top level architecture of the LSD block is presented in Fig. 15 for 2×2 real-valued system and QPSK. The principle is the same for the other antenna setups and modulation scheme combinations. There are $s = 2N, N = N_{\mathrm{T}} = N_{\mathrm{R}}$ stages with PED computation and three sorters. The $\mathbf{R}s$ represents the results from the $\mathbf{Rx}$ block for stage s with size $1 \times s\Omega_r$, where $\Omega_r = 2^{Q/2}$. The first level of the LSD is simple and consists only of multiplications and additions, performed in parallel. The number of adders depends on the size of the $\mathbf{R}s$. With 4×4, QPSK and $K = 8$, the sorter is needed only after the third stage. In the insertion sorter, the PEDs are stored in a shift register and as a new Euclidean distance is computed, it is compared to the existing values in the register and the register is shifted if the new value is smaller than the existing value. The LLRs are computed from the list of candidates and PEDs.

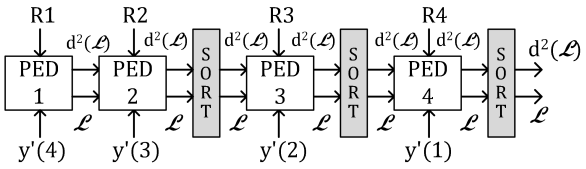

Fig. 15 The top level architecture of the LSD block for 2×2 system and QPSK.

4.1.2 ASIC Synthesis Results

In the implementation results, pipelining of subcarriers is used if possible, so that the detection of the next subcarrier can begin already when the first subcarrier is being detected. An example is shown in Fig. 16 for the K-best LSD with $K = 8$ and QPSK in the 4×4 system. The LLR computation is the slowest block. The first three stages in the LSD do not need sorters due to QPSK modulation, and can therefore be performed in one clock cycle (cc). As a result of pipelining, the slowest block in the detector creates a bottleneck and its latency is used as D_{tp} in (6) and denoted as throughput latency in the synthesis results.

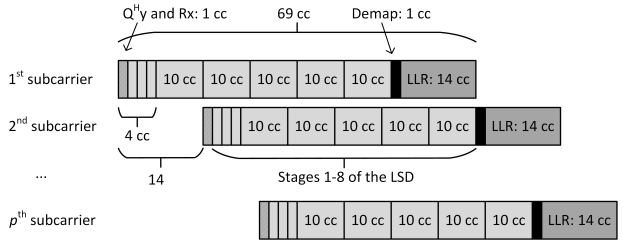

Fig. 16 The timing and latencies of the K-best LSD with $K = 8$ and QPSK in the 4×4 system.

The implementation results for the K-best LSD with list sizes 8 and 16 are presented in Table 2. The results for the whole detector include both, the white and the grey boxes in the block diagram in Fig. 14. The modulation order and list size have a great impact on the latency and complexity of the K-best LSD. With the QPSK, the K-best LSD is able to achieve the required detection rate, even with the list size of 16. As the modulation order increases to 64-QAM, the latency increases also and the required detection rate cannot be met. The 16-best LSD is able to fulfill the detection rate requirement only with 4×4 system and QPSK. For other combinations of the modulation order and number of antennas, the latency is too high because the used HLS tool was unable to create a better architecture with the given clock frequency. For example, in the case of $K = 8$, 64-QAM and 8×8 system, the LLR, $\mathbf{Rx}$, and PED computations can be parallelized better and the throughput latency decreases to 54 cc, if the clock frequency is decreased to 667 MHz. This equals detection rate of 593 Mbps. However, even this is not enough to fulfill the detection rate requirement of 696 Mbps and lower clock frequency and more parallelism are needed if possible.

4.2 LMMSE Detector

4.2.1 Architecture

The $\mathbf{Q}$ and $\mathbf{R}$ matrices are used to compute the LMMSE filter $\mathbf{W}$ as shown in Fig. 17. Again, the operations performed for every subcarrier are inside the grey boxes, and the operations computed only once in a channel coherence time are in the white boxes.

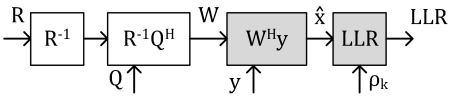

Fig. 17 The top-level architecture of the LMMSE receiver.

The inversion of the $\mathbf{R}$ can be computed using the algorithm presented in [33]. Only adders and multipliers are needed for the $\mathbf{R}^{-1}\mathbf{Q}^{\text{H}}$ and $\mathbf{W}^{\text{H}}\mathbf{y}$ blocks, and their number depends on the number of antennas. All the operations in the matrix-vector multiplication block $\mathbf{W}^{\text{H}}\mathbf{y}$ can be performed in parallel. The LLR computation is implemented using an approximated log-likelihood criterion [34]. The post-processing signal-to-interference-plus-noise ratio (SINR) ρ_k of layer k and Gray-labeling of signal points are exploited instead of computing the Euclidean distances between the detected signal $\hat{\mathbf{x}}$, and the candidate symbols. The multiplications with a power of two are calculated as shifts.

4.2.2 ASIC Synthesis Results

The ASIC implementation results for the LMMSE detector are presented in Table 2. Similar pipelining of subcarriers is used as with the K-best LSD. The latency of the LMMSE detector in the 4×4 system was possible to get as low as 35 or 40 cc, depending on the modulation order. However, the gate count would have been more than tripled and power consumption would have been quadrupled. The inversion of $\mathbf{R}$ is the most time consuming part in the LMMSE detector. It needs to be computed only once in a channel coherence time, and therefore its latency was increased to lower the power consumption without degrading the throughput latency.

Table 2 The ASIC Synthesis Results

	The whole detector			**W** and **Rx** computation excluded			
Detector	Gates (kGE)	Power (mW)	Latency (cc)	Energy/bit (pJ/bit)	Throughput latency (cc)	Detection rate (Mbps)	Required rate (Mbps)
4-QAM 4×4							
LMMSE	335	42.1	225	3.1	1	6154	
8-best LSD	136	44.6	69	87.7	14	440	116
16-best LSD	172	53.8	93	150.5	18	342	
16-QAM 4×4							
LMMSE	364	46.5	230	14.3	6	2051	
8-best LSD	243	75.9	91	108.8	22	559	232
16-best LSD	278	92.2	544	549.6	97	127	
64-QAM 4×4							
LMMSE	407	52.0	230	13.7	6	3077	
8-best LSD	611	219.8	499	343.7	76	243	348
16-best LSD	528	187.3	1001	757.4	161	115	
4-QAM 8×8							
LMMSE	776	124.3	2314	98.2	12	1026	
8-best LSD	426	152.1	165	213.3	22	559	232
16-best LSD	347	112.6	1060	941.8	81	152	
16-QAM 8×8							
LMMSE	787	132.9	2314	50.4	12	2051	
8-best LSD	941	304.1	240	324.7	38	648	464
16-best LSD	642	197.5	1438	832.7	97	254	
64-QAM 8×8							
LMMSE	1039	153.8	2314	59.5	12	3077	
8-best LSD	1040	338.6	1895	657.6	98	377	696
16-best LSD	1242	408.4	2494	1496.9	177	209	

The throughput latency for the LMMSE detector is low, because only the LLR computation and the multiplication of the received signal with the filter are performed for every subcarrier. Hence, the detection rate requirement can be met even in the 8×8 system.

In terms of detection rate and energy efficiency, the LMMSE detector would be the optimal choice even though the LMMSE filter computation is time consuming. For example, in the 8×8 system with 64-QAM, 2.4 GHz center frequency and 20 MHz bandwidth, the LMMSE detector is able to process 282 TTIs at 3 km/h mobile speed and 8 TTIs at 100 km/h during channel coherence time. With similar assumptions, the 8-best LSD would be able to process 34 TTIs at 3 km/h and 1 TTI at 100 km/h. One TTI at 20 MHz bandwidth consists of 14400 data subcarriers taking the pilot overhead into account. The PED computation and sorting operations are time consuming in the K-best LSD and have to be performed for every subcarrier, whereas the slowest operation in the LMMSE detector needs to be performed only once in a channel coherence time.

5 Performance–Energy Efficiency and Performance–Complexity Comparison

The simulation and implementation results are combined and the goodput as a function of the energy efficiency and the gate count is presented. The 20 MHz bandwidth is considered when computing the goodput.

The goodput as a function of energy efficiency is illustrated in Fig. 18 for the 4×4 system and different correlation scenarios. Clearly the LMMSE detector has the best energy efficiency, but cannot provide similar goodput as the K-best LSD in the correlated scenarios. In an uncorrelated channel with QPSK, the LMMSE detector provides highest goodput at 0 dB SNR, but requires 8 dB SNR in a highly correlated channel to reach similar goodput. K-best LSD, on the other hand, is able to handle the highly correlated channel and outperforms the LMMSE detector. In a moderately correlated channel at 14 dB SNR, the QPSK reaches better goodput than the 16-QAM with better energy efficiency for all detectors. Again, at 12 dB SNR in an uncorrelated channel with 16-QAM, the LMMSE detector provides similar throughput as the K-best LSD, but in a moderately correlated channel 20 dB SNR is needed to reach the same throughput with the LMMSE detector. In a moderately correlated channel with 64-QAM at 24 dB SNR, the 16-best LSD has the highest goodput, but as the SNR is increased to 30 dB, the detection rate limits the goodput of the 16-best LSD, making it the worst choice in terms of both, goodput and energy efficiency.

The goodput as a function of the gate count is illustrated in Fig. 19 for the 4×4 system in different

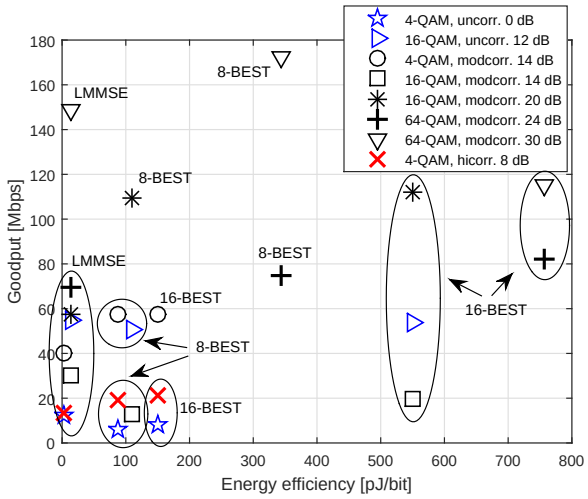

Fig. 18 Goodput vs. energy efficiency for the 4×4 system.

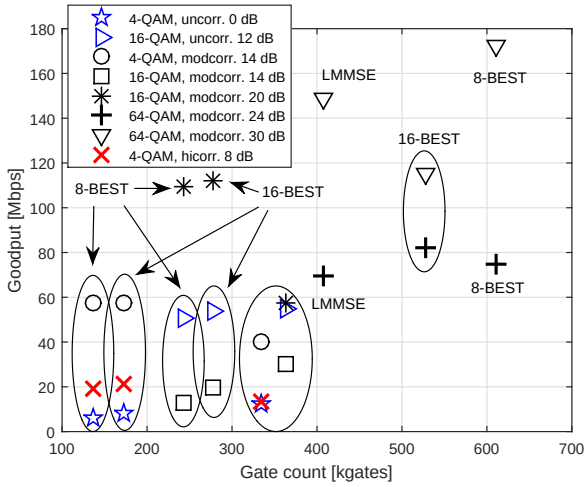

Fig. 19 Goodput vs. gate count for the 4×4 system.

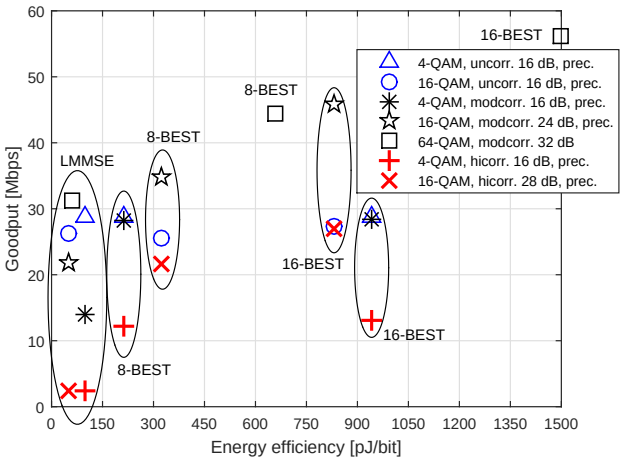

Fig. 20 Goodput vs. energy efficiency for the 8×8 system.

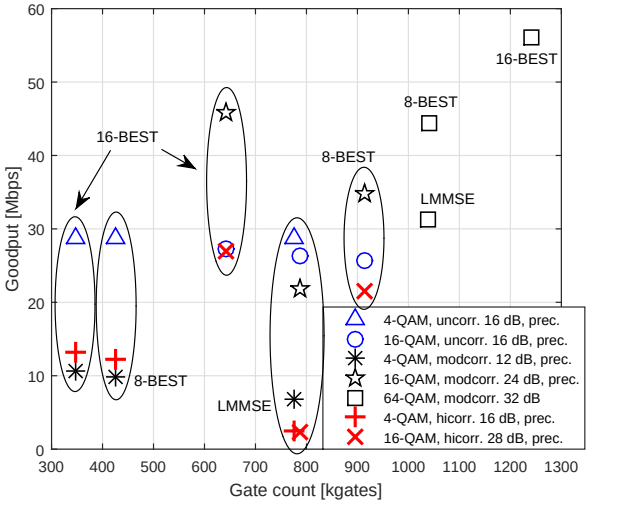

Fig. 21 Goodput vs. gate count for the 8×8 system.

correlation scenarios. The LMMSE detector requires a high gate count due to the LMMSE filter computation, but the modulation order has only a small impact on it. The K-best LSD, on the other hand, has a smaller gate count with QPSK and 16-QAM. Here we consider the power consumption to be a more important factor than the complexity, when evaluating the implementation aspects of the algorithms, but in real life devices, the chip area is limited and has to be taken into account when designing the wireless receiver.

The goodput as a function of energy efficiency is illustrated in Fig. 20 and as a function of gate count in Fig. 21 for the 8×8 system and different correlation scenarios. As in the 4×4 system, the LMMSE detector has the best energy efficiency and quite high gate count. The goodput is computed with QPSK, precoding and 16 dB SNR for all correlation scenarios, and it is clear that the uncorrelated channel is most suitable for the LMMSE detector. With moderate correlation and the same SNR, the K-best LSD can reach similar goodput as in uncorrelated channel, but with the LMMSE detector the goodput is approximately halved. The list size does not have a major impact on the performance or complexity of the K-best LSD with QPSK, but affects the energy efficiency significantly. With 64-QAM the LMMSE detector cannot compete with the K-best LSD in terms of goodput or gate count, but the energy efficiency is superior. The low modulation orders could have a large list size in terms of gate count, but when the energy efficiency is also taken into account, $K = 8$ would be the better choice. The energy efficiency of the LMMSE detector is superior, but there are only few occasions where it is able to outperform the K-best LSD and requires large area.

The K-best detector with $K = 16$ is clearly too complex and energy inefficient for handheld devices in relation to the goodput it is able to provide with the 28 nm CMOS technology. As a conclusion, the list size of 16 is unnecessarily large for the 4×4 system. It can offer improved data transmission throughput with high modulation order, particularly when the spatial correlation of the channel increases, but the improved performance comes with the cost of significantly worse energy efficiency and higher complexity. In the 8×8 system, the 16-best LSD can compete in terms of gate count and performance, but the energy efficiency is poor.

If the receiving device is, for example, a laptop, and does not have to monitor power consumption as carefully as handheld devices, the 16-best algorithm could be used in challenging channel conditions with high modulation orders. It has to be noted that the hardware detection rate of the 16-best LSD can be quite poor and limit the performance, even when the channel conditions would be favorable for high data transmission throughput.

The results are obtained using one clock frequency for all algorithms, because the generation of several clock signals increases power consumption. Lower clock frequency could enable more parallelism and faster scheduling for some algorithms, such as the 16-best LSD, but does not necessarily guarantee a better detection rate. Also the area and energy efficiency results would be affected. One option to optimize the latency of the algorithms would be to choose clock frequency for each algorithm separately, but this requires generation of different clock signals, which increases energy consumption.

6 Conclusions

The detectors with the best goodput at 20 MHz bandwidth in different correlation scenarios with the given SNR are presented in Tables 3 and 4 for the 4×4 and 8×8 systems, respectively. Cases with and without precoding are considered. The modulation order is given in parenthesis. If the goodput difference between detectors is no more than 3 Mbps, the one with better energy efficiency is chosen.

It can be noted that even though the LMMSE detector can outperform the K-best LSD with certain modulation orders in the low SNR regime (for example the 16-QAM in a moderately correlated channel and 4×4 system in Fig. 6), in that same SNR regime the K-best LSD with a lower modulation order (QPSK) can provide higher throughput, and is therefore chosen instead of the LMMSE detector (in this example the detection rate is always greater than the throughput and therefore the goodput equals the data transmission throughput). If only one modulation order was used for transmission on the whole SNR regime, the LMMSE detector could be used, for example, in a moderately correlated channel at 10 to 15 dB with 16-QAM, 4×4 system and precoding.

The transmit precoding increases the data transmission throughput at the low SNR regime, especially for the LMMSE detector. This means that there are more possibilities to use the simple LMMSE detector to decrease power consumption. It should also be noted that due to the used precoding adaptation method, the precoder sometimes degrades the goodput at high SNR, which can affect the results, especially for the 8×8 system.

Table 3 The Recommended Detector in the 4×4 System

SNR	Uncorr.	Mod. corr.	High corr.
4×4 no precoding			
2 dB	LMMSE (4)	-	-
10 dB	LMMSE (4)	8-best (4)	8-best (4)
15 dB	8-best (16)	8-best (4)	8-best (4)
20 dB	16-best (64)	8-best (16)	8-best (4)
30 dB	LMMSE (64)	8-best (64)	8-best (16)
4×4 precoding			
2 dB	LMMSE (4)	LMMSE (4)	LMMSE (4)
10 dB	LMMSE (4)	8-best (4)	8-best (4)
15 dB	8-best (16)	8-best (4)	8-best (4)
20 dB	LMMSE (64)	8-best (16)	8-best (4)
30 dB	LMMSE (64)	8-best (64)	8-best (16)

Table 4 The Recommended Detector in the 8×8 System

SNR	Uncorr.	Mod. corr.	High corr.
8×8 no precoding			
4 dB	-	-	-
10 dB	8-best (4)	8-best (4)	-
15 dB	8-best (4)	8-best (4)	8-best (4)
20 dB	8-best (16)	LMMSE (4)	8-best (4)
30 dB	LMMSE (64)	8-best (16)	16-best (16)
8×8 precoding			
4 dB	LMMSE (4)	-	-
10 dB	8-best (4)	LMMSE (4)	-
15 dB	8-best (4)	8-best (4)	8-best (4)
20 dB	8-best (16)	8-best (4)	8-best (4)
30 dB	8-best (64)	8-best (16)	16-best (16)

The performance and implementation results of this paper demostrate that the LMMSE detector can mainly be used in an uncorrelated channel. In other scenarios, the K-best LSD is required to guarantee more reliable transmission. The use of more accurate channel estimation method, such as the MMSE filtering of the LS

estimates, and different mobile speeds could change the situation.

Only in a few occasions, the 16-best LSD outperforms the 8-best LSD. In the case of the 4×4 system without precoding and an uncorrelated channel at 20 dB, the difference between the 16-best LSD and LMMSE detector is only slightly over 3 Mbps. In the 8×8 system with high correlation at 30 dB, the difference between list sizes 8 and 16 is significant, which can also be observed in Fig. 10.

We have considered the case where all the possible transmit antennas are used with the lowest code rate defined in the LTE standard. The use of transmission adaptation, where the modulation, coding and rank scheme (MCRS) is adapted based on the channel condition, can bring new perspective to adaptive detection. The modulation scheme providing the best performance at a certain SNR value is chosen every time for transmission in Tables 3 and 4. Therefore, the K-best LSD algorithm is mainly used. This means high power consumption especially with the higher modulation orders. However, as we have proposed in [35], the receiver could choose to prefer the QPSK and 16-QAM constellations and inform the transmitter to avoid the use of 64-QAM in transmission adaptation. This would improve the energy efficiency, especially when the K-best detector is used. The avoidance of 64-QAM is possible because when the 16-QAM and QPSK constellations are combined with a suitable coding rate and transmission rank, a similar throughput as with a MCRS using 64-QAM can be reached. However, this requires that the receiver is able to handle higher coding rates. Also the maximum data transmission throughput at high SNRs can be reached only with the 64-QAM, in which case the use of 64-QAM would be mandatory.

The main motivation for the adaptive detection is the decreased energy consumption. The batteries of the current mobile terminals seem to run out quickly, and adding support for more than two antenna elements increases the energy consumption even further, necessitating the use of power saving methods. Adaptive detection is one solution to enable energy efficient detection at the receiver. Two detector algorithms could be produced on one chip and depending on the channel conditions, the more suitable algorithm is chosen. In the case of the K-best and LMMSE detectors, there are some blocks that have similar computations, such as the matrix multiplications, which could be shared between the algorithms to decrease the chip area.

The detection algorithm selection criteria were not discussed. Popular methods in the literature include computation of the condition number or some other metric [3,36]. Computation of a separate metric for detector adaptation would require an extra calculation block in the receiver, increasing the area and power consumption. Therefore, some already existing method used in the wireless receiver should be used if possible. The impact of the power and cost of the QRD, HARQ, Turbo decoding and computation of the detection algorithm selection criteria on the adaptive detection would be an interesting study item in the future. It could also be studied how an adaptive system with two detector algorithms compares to a system using only the simple LMMSE detection algorithm or a system with the K-best LSD algorithm with one or more list sizes.

References

1. 3rd Generation Partnership Project (3GPP); Technical Specification Group Radio Access Network, "Evolved universal terrestrial radio access E-UTRA; physical channels and modulation (release 10) TS 36.211 (version 10.0.0)," Tech. Rep., 2010.
2. E. N. Onggosanusi, A. G. Dabak, and S. Hosur, "Multimode detection," Patent U.S. 2006/0018410 A1, Jan. 2006.
3. H. Shen, H. Zhang, and C. Zhao, "An efficient adaptive receiver for MIMO–OFDM systems," in *Proc. Int. Conf. on Wireless Commun. and Sign. Proc.*, Nanjing, China, Nov. 9–11 2011, pp. 1–5.
4. X. Chen, A. Minwegen, Y. Hassan, D. Kammler, S. Li, T. Kempf, A. Chattopadhyay, and G. Ascheid, "FLEXDET: Flexible, efficient multi-mode MIMO detection uding reconfigurable ASIP," in *Proc. Int. Symb. on Field-progr. Custom Comp. Machines*, vol. 3, 2012, pp. 69–76.
5. X. Chen, A. Minwegen, S. B. Hussain, A. Chattopadhyay, G. Ascheid, and R. Leupers, "Flexible, efficient multimode MIMO detection by using reconfigurable ASIP," *IEEE Trans. VLSI Syst.*, vol. 23, no. 10, pp. 2173–2186, Oct. 2015.
6. F. Sheikh, C.-H. Chen, D. Yoon, B. Alexandrov, K. Bowman, A. Chun, H. Alavi, and Z. Zhang, "3.2 Gbps channel-adaptive configurable MIMO detector for multimode wireless communication," in *Proc. IEEE Works. on Sign. Proc. Syst.*, Belfast, Northern Ireland, Oct. 20–22 2014, pp. 1–6.
7. 3rd Generation Partnership Project (3GPP); Technical Specification Group Radio Access Network, "Evolved universal terrestrial radio access E-UTRA; physical layer procedures (release 11) TS 36.213 (version 11.2.0)," Tech. Rep., 2013.
8. S. Yoshizawa, N. Miyazaki, D. Nakagawa, and Y. Miyanaga, "A low-power adaptive MIMO detector for MIMO–OFDM WLAN systems," in *Proc. Annual Conf. Asia-Pacific Signal and Information Processing Association*, Xi'an, China, Oct. 18–21 2011, pp. 2486–2489.
9. E. Suikkanen and M. Juntti, "Study of adaptive detection and channel estimation for MIMO–OFDM systems," *Springer Wireless Pers. Commun.*, Dec. 2014.
10. E. Suikkanen, J. Janhunen, S. Shahabuddin, and M. Juntti, "Study of adaptive detection for MIMO–OFDM systems," in *Proc. Int. Symp. on System-on-Chip*, Tampere, Finland, Oct. 23–24 2013, pp. 1–4.

11. E. Suikkanen, J. Ketonen, and M. Juntti, "Detection and channel estimation in 8 × 8 MIMO–OFDM," in *Proc. IEEE Int. Conf. Cognitive Radio Oriented Wireless Networks and Communications*, Oulu, Finland, Jun. 2–4 2014, pp. 299–304.
12. E. Suikkanen and M. Juntti, "ASIC implementation and performance comparison of adaptive detection for MIMO–OFDM system," in *Proc. Annual Asilomar Conf. Signals, Syst., Comp.*, Pacific Grove, USA, Nov. 8–11 2015, pp. 1632–1636.
13. H. Artes, D. Seethaler, and F. Hlawarsch, "Efficient detection algotihms for MIMO channels: A geometrical approach to approximate ML detection," *IEEE Trans. Signal Processing*, vol. 51, no. 11, pp. 2808–2820, Nov. 2003.
14. K. Wong, C. Tsui, R.-K. Cheng, and W. Mow, "A VLSI architecture of a K-best lattice decoding algorithm for MIMO channels," in *Proc. IEEE Int. Symp. on Circuits and Systems*, vol. 3, Scottsdale, AZ, May 26–29 2002, pp. 273–276.
15. A. Burg, M. Borgmann, M. Wenk, M. Zellweger, W. Fichtner, and H. Bölcskei, "VLSI implementation of MIMO detection using the sphere decoding algorithm," *IEEE J. Solid-State Circuits*, vol. 40, no. 7, pp. 1566–1577, Jul. 2005.
16. L. G. Barbero and J. S. Thompson, "FPGA design considerations in the implementation of a fixed-throughput sphere decoder for MIMO systems," in *Int. Conf. on Field Programmable Logic and Applications*, Sydney, Australia, Aug. 28–30 2006, pp. 1–6.
17. B. Wu and G. Masera, "Efficient VLSI implementation of soft-input soft-output fixed-complexity sphere decoder," *IET Communications*, vol. 6, no. 9, pp. 1111–1118, 2012.
18. M. Myllylä, M. Juntti, and J. Cavallaro, "Implementation aspects of list sphere decoder algorithms for MIMO–OFDM systems," *Signal Processing, Elsevier*, vol. 90, no. 10, pp. 2863–2876, 2010.
19. D. Wübben, R. Böhnke, V. Kühn, and K. Kammeyer, "MMSE extension of V-BLAST based on sorted QR decomposition," in *Proc. IEEE Veh. Technol. Conf.*, vol. 1, Orlando, Florida, USA, Oct. 6–9 2003, pp. 508–512.
20. M. K. Ozdemir and H. Arslan, "Channel estimation for wireless OFDM systems," *IEEE Communications Surveys & Tutorials*, vol. 9, no. 2, pp. 18–48, 2007.
21. M. Meidlinger and Q. Wang, "Performance evaluation of LTE advanced downlink channel estimation," in *Proc. Int. Conf. on Syst., Sign. and Image Proc.*, Vienna, Austria, Apr. 11–13 2012, pp. 252–255.
22. S. Lin, D. J. Costello Jr, and M. J. Miller, "Automatic-repeat-request error-control scheme," *IEEE Trans. Magn.*, vol. 22, no. 12, Dec. 1984.
23. D. Chase, "Code combining – a maximum-likelihood decoding approach for combining an arbitrary number of noisy packets," *IEEE Trans. Commun.*, vol. 33, no. 5, pp. 385–393, May 1985.
24. ZTE, "R1-091716 DL codebook design for 8 Tx MIMO in LTE-A," 3rd Generation Partnership Project (3GPP) TSG RAN WG1 Meeting 57, San Francisco, USA, Tech. Rep., May 2009.
25. 3rd Generation Partnership Project (3GPP); Technical Specification Group Radio Access Network, "Radio transmission and reception (3G TS 45.005 version 5.4.0 (release 5))," 3rd Generation Partnership Project (3GPP), Tech. Rep., 2002.
26. Cadence Design Systems Datasheet, "Cadence C-to-silicon compiler," [Online]. Available: http://www.cadence.com/products/sd/silicon_compiler/pages/default.aspx, accessed: Mar. 17, 2016.
27. Synopsys Design Compiler Datasheet, "Synopsys design compiler 2010," [Online]. Available: http://www.synopsys.com/Tools/Implementation/RTLSynthesis/Pages/default.aspx, accessed: Mar. 17, 2016.
28. J. Ketonen, M. Juntti, and J. R. Cavallaro, "Performance-complexity comparison of receivers for a LTE MIMO–OFDM system," *IEEE Trans. Signal Processing*, vol. 58, no. 6, pp. 3360–3372, Jun. 2010.
29. B. Gestner and D. V. Anderson, "Single Newton-Raphson iteration for integer-rounded divider for lattice reduction algorithms," in *IEEE 51st Midwest Symp. on Circ. and Syst.*, vol. 2, Knoxville, TN, USA.
30. G. H. Golub and C. F. Van Loan, *Matrix Computations, 3rd ed.* Baltimore: The Johns Hopkins University Press, 1996.
31. M. O. Damen, H. El Gamal, and G. Caire, "On maximum–likelihood detection and the search for the closest lattice point," *IEEE Trans. Inform. Theory*, vol. 49, no. 10, pp. 2389–2402, Oct. 2003.
32. M. Myllylä, J. Antikainen, M. Juntti, and J. R. Cavallaro, "The effect of LLR clipping to the complexity of list sphere detector algorithms," in *Proc. Annual Asilomar Conf. Signals, Syst., Comp.*, Pacific Grove, USA, Nov. 4-7 2007, pp. 1559–1563.
33. A. El-Amawy and K. R. Dharmarajan, "Parallel VLSI algorithm for stable inversion of dense matrices," *Computers and Digital Techniques, IEE Proceedings E*, vol. 136, no. 6, pp. 575–580, Nov. 1989.
34. I. Collings, M. R. G. Butler, and M. McKay, "Low complexity receiver design for MIMO bit-interleaved coded modulation," in *Proc. IEEE Int. Symp. Spread Spectrum Techniques and Applications*, Sydney, Australia, Aug. 30 –Sep. 2 2004, pp. 1993–1997.
35. E. Suikkanen, J. Ketonen, and M. Juntti, "Transmission adaptation," International PCT Patent Application No. PCT/EP2012/066573, Aug. 2012.
36. J. Maurer, G. Matz, and D. Seethaler, "Low-complexity and full-diversity MIMO detection based on condition number thresholding," in *Proc. IEEE Int. Conf. Acoust., Speech, Signal Processing*, vol. 3, Honolulu, Hawaii, USA, Apr. 15–20 2007, pp. 61–64.